Chemical Science

ROYAL SOCIETY OF CHEMISTRY

EDGE ARTICLE

View Article Online
View Journal | View Issue

Cite this: *Chem. Sci.*, 2025, **16**, 16597

All publication charges for this article have been paid for by the Royal Society of Chemistry

Comparison of Ce(IV)/Th(IV)-alkynyl complexes and observation of a *trans*-influence ligand series for Ce(IV)

Qiaomu Yang, †[a] Xiaojuan Yu, [b] Ekaterina Lapsheva, ‡[a] Pragati Pandey, §[a] Patrick W. Smith, [c] Himanshu Gupta, [a] Michael R. Gau,[a] Patrick J. Carroll,[a] Stefan G. Minasian, [c] Jochen Autschbach *[b] and Eric J. Schelter *[ade]

Organometallic cerium(IV) complexes have been challenging to isolate and characterize due to the strongly oxidizing nature of the cerium(IV) cation. Herein, we report two cerium(IV) alkynyl complexes, [Ce(TriNOx)(C≡C-SiMe$_3$)] (**1-Ce^{TMS}**) and [Ce(TriNOx)(C≡C-Ph)] (**1-Ce^{Ph}**) (TriNOx^{3-} = *tris*(2-*tert*-butylhydroxylaminato)benzylamine), that include terminal alkyne moieties. The isostructural thorium analogue [Th(TriNOx)(C≡C-SiMe$_3$)] (**1-Th^{TMS}**) was also synthesized and compared with **1-Ce^{TMS}** in bond distance, ^{13}C-NMR spectra, vibrational spectra and electronic structure. The Ce–C bond distances were 2.501(3) Å for **1-Ce^{Ph}** and 2.513(5) Å for **1-Ce^{TMS}** on the shorter end of the few reported Ce^{IV}–C single bonds (2.478(3)–2.705(2) Å), possibly indicating significant Ce 5d- and 4f-orbital involvement. ^{13}C-NMR spectroscopy was also consistent with Ce–C covalency, with significantly deshielded resonances ranging from 185–213 ppm. Such ^{13}C-NMR shifts demonstrate a strong influence from spin–orbit coupling (SOC) effects, corroborated by computational studies. Raman analysis showed $\nu_{C\equiv C}$ stretching frequencies of 2000 cm^{-1} (**1-Ce^{TMS}**) and 2052 cm^{-1} (**1-Ce^{Ph}**), indicating the cerium(IV)–alkynyl interaction, compared to the parent HC≡CPh (IR = 2105 cm^{-1} and Raman = 2104 cm^{-1}). L$_3$-edge X-ray absorption measurements revealed a predominant Ce(IV) electronic configuration, and magnetic measurements revealed temperature-independent paramagnetism. Electrochemical studies similarly revealed the electron donating ability of the alkynyl ligands, stronger than either fluoride or imido ligands for the Ce(IV)(TriNOx)-framework, with a cerium(IV/III) reduction potential of E_{pc} = −1.58 to −1.66 V *vs.* Fc/Fc$^+$. Evidence for a *trans*-influence has been observed by evaluating a series including previously reported [Ce^{IV}(TriNOx)X]$^{+/0}$ complexes with axial ligands X = THF, I$^-$, Br$^-$, Cl$^-$, F$^-$, $^-$C≡C-Ph, $^-$C≡C-SiMe$_3$, $^-$NH(3,5-(CF$_3$)$_2$-Ar), $^-$OSiPh$_3$, $^-$N(M(L))(3,5-(CF$_3$)$_2$-Ar) [M(L) = Li(TMEDA), K(DME)$_2$ or Cs(2,2,2-crypt)]. These data stand in contrast with previous reports of an inverse *trans*-influence at cerium(IV) and point to differences in involvement of cerium 4f- *versus* 5d-orbitals in the electronic structures of the complexes.

Received 3rd May 2025
Accepted 5th August 2025

DOI: 10.1039/d5sc03222a

rsc.li/chemical-science

Introduction

The bonding interactions between f-block elements and organic fragments are of significant interest due to often complex 4f/5f- and 5d/6d-orbital involvement resulting in variable, partially covalent metal–ligand interactions.[1–5] Modern spectroscopic and computational techniques have contributed fruitful studies on this topic.[6,7] Such studies help delineate the similarities and differences between bonding in lanthanide, actinide, and d-block metal compounds for applications in reactivity, separations chemistry, and others.[4,8–10] A key avenue for exploring f-/d-bond covalency is the study of high oxidation state compounds, where the high charge on the metal cation can promote orbital overlap with varied contributions from 4/5f- and 5/6d-manifolds. Such studies require attaining stable complexes in high oxidation states with spectroscopically active ligands for

[a]*P. Roy and Diana T. Vagelos Laboratories, Department of Chemistry, University of Pennsylvania, 231 S. 34th St., Philadelphia, PA 19104, USA. E-mail: schelter@sas.upenn.edu*

[b]*Department of Chemistry, University at Buffalo, State University of New York, 732 Natural Sciences Complex, Buffalo, NY 14260, USA. E-mail: jochena@buffalo.edu*

[c]*Lawrence Berkeley National Laboratory, 1 Cyclotron Rd, Berkeley, CA 94720, USA*

[d]*Department of Chemical and Biomolecular Engineering, University of Pennsylvania, 220 S. 33rd St., 311A Towne Building, Philadelphia, PA, 19104, USA*

[e]*Department of Earth and Environmental Science, University of Pennsylvania, 251 Hayden Hall, 240 South 33rd Street, Philadelphia, PA, 19104, USA*

† Current address: 9700 S. Cass Avenue, The Center of Nanoscale Materials, Argonne National Lab, IL 60439 (USA).

‡ Current address: 410 Forest Ave, Sheboygan Falls, Ereztech Labs, WI 53085.

§ Current address: Group of Coordination Chemistry, Institut des Sciences et Ingénierie Chimiques, École Polytechnique Fédérale de Lausanne (EPFL), CH-1015 Lausanne, Switzerland.

study.[6,11] In lanthanide chemistry, the most accessible element in this context is cerium(IV). Our group, along with others, has devoted effort to realizing organometallic compounds featuring Ce(IV)–carbon bonds. These studies explored the redox properties and spectroscopic features, together with electronic structure calculations, to model the unique physicochemical signatures and analysis of f-element bond covalency.[1,2,12–18]

Organo-cerium(IV) complexes are generally rare,[2] and their scarcity is likely due to redox chemistry, with carbanions prone to oxidation and cerium(IV) cations prone to reduction. Notable examples in the field include metallocene Ce(IV) complexes, heteroatom-stabilized Ce(IV)–C compounds, and Ce(IV) complexes with monodentate carbanion ligands. Metallocene complexes include cerium(IV) cyclopentadienides,[19,20] cerium(IV) cyclooctatetraenes such as $[Ce(COT)_2]$,[15,21–23] or cerium(IV) bispentalenides, with important examples reported between 1976 and 2010.[24] Progress has also been made in heteroatom-stabilized cerium(IV)–carbon complexes. Furthermore, Arnold and coworkers reported the use of N-heterocyclic carbene ligands featuring Ce^{IV}–C_{sp^2} bonds in 2009,[25] and Liddle and coworkers studied the bis(iminophophorano)methandiide (BIPM) ligand in $[Ce^{IV}(BIPM^{TMS})_2]$ featuring a Ce^{IV}–C_{sp^2} bond in 2013 (Fig. 1).[3,14] Our group reported $[Ce^{IV}(\kappa^2\text{-}ortho\text{-oxa})(MBP)_2]^-$ in 2021,[2] where *ortho*-oxa = dihydrodimethyl-2-[4-(trifluoromethyl)phenyl]-oxazolide and MBP = 2,2′-methylenebis(6-*tert*-butyl-4-methylphenolate). The complex featured a Ce^{IV}–aryl (C_{sp^2}) bond supported by a chelating oxazolide group. Recent progress has been made in Ce–C single bond chemistry, without supporting chelating groups using monodentate supporting ligands. Chen, Li, Tamm, *et al.* recently used an imidazolin-2-iminato (ImN^-) ligand featuring a Ce^{IV}–alkynyl (C_{sp}) bond in $[Ce^{IV}(C{\equiv}C\text{-}Ph)(ImN)_3]$ complexes in 2024.[26] In the same work, the team also realized compounds featuring Ce^{IV}–aryl (C_{sp^2}) and Ce^{IV}–alkyl (C_{sp^3}) bonds. Independently and at the same time, La Pierre and co-workers employed a tri-*tert*-butyl imidophosphorane ligand on $[Ce^{IV}(Alkyl)(NP(tert\text{-}butyl)_3)_3]$ featuring Ce^{IV}–alkyl (C_{sp^3}) bonds, where alkyl is neopentyl (Npt) or benzyl (Bn).[27] Furthermore, a Ce^{IV}–cyclopropenyl complex featuring a Ce^{IV}–C_{sp^2} bond and ring-open isomerization was recently disclosed by us.[28]

In pursuit of cerium(IV) organometallic complexes, three primary synthetic strategies have been employed: the use of a supporting ligand with electron-donating groups to stabilize the Ce^{IV} oxidation state, the use of multidentate ligands with both a carbanion and electronically supporting heteroatoms coordinating to the Ce^{IV} cation, and tethering of ligands with a steric bulk to kinetically inhibit the homolysis of the Ce^{IV}–C bond.[2] In this study, we sought to employ the first strategy to further expand the scope of Ce^{IV}–C chemistry and realize Ce^{IV}–alkynyl complexes. The $TriNOx^{3-}$ ligand has been used by us for the stabilization of the Ce(IV) oxidation state and a series of $[Ce^{IV}(TriNOx)X]^{+/0}$ axial complexes, X = THF, I^-, Br^-, Cl^-, F^-,[29] anilide,[12] imide,[6,12,13,30] siloxide,[13] carbamate,[30] and oxo,[6,13] were synthesized previously. For the current work, H–C≡C-$SiMe_3$ and H–C≡C-Ph have been used as two alkyne precursors. As a result, compounds with Ce^{IV}–C_{sp} bonds were obtained without heteroatom stabilization and without steric hindrance provided by bulky substituents. This approach also provided the opportunity for a more direct analysis of the cerium(IV)–carbon bonding interactions without the influence of conjugated heteroatoms.

Herein, we report the isolation of Ce(IV)–C_{sp} compounds with terminal carbon atom coordination (Fig. 1). The complexes provide opportunities for spectroscopic characterization of the –C≡C– vibrations and electronic structure calculations. The observed ^{13}C-NMR chemical shifts of the title compounds are remarkably downfield because of effects originating from the relativistic spin–orbit interaction. The alkynyl moiety is also found to be a strong donor for stabilizing cerium(IV) with metal redox potentials of −1.49 and −1.57 V *vs.* Fc/Fc^+ (Fc = $Fe(C_5H_5)_2$). The information obtained in the present study has been applied to complete a *trans* influence series for related $[Ce^{IV}(TriNOx)X]^{+/0}$ complexes with axial ligands X including THF, halide, alkynyl, amide, siloxide, and imide ligands. These results provide important opportunities for improving our understanding of the bonding involving lanthanides in high oxidation states.

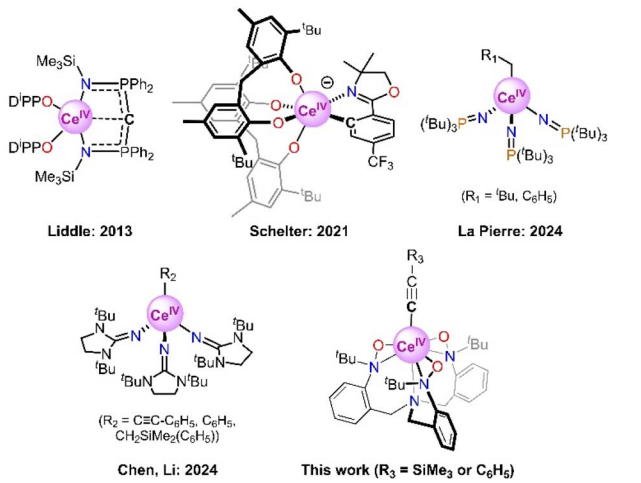

Fig. 1 Recent examples of cerium(IV)–carbon containing complexes, including heteratom-stabilized Ce(IV) compounds, or Ce(IV) complexes with monodentate carbanion ligands.

Results and discussion

Synthesis of cerium(IV) and thorium(IV) alkynyl complexes

The precursor complex $[Ce^{IV}(TriNOx)Cl]$ (1-Ce^{Cl}) was obtained by mixing $[Ce^{III}(TriNOx)(THF)]$ with CPh_3Cl in Et_2O in a modified reaction based on previous reports,[29] where the purple solid product precipitates immediately, with a simple workup and high (90%) yield. Addition of a dark purple solution of [Ce(TriNOx)Cl] in CH_2Cl_2 to a colorless solution of Li–C≡C-Ph (1.6 equiv.) in a toluene/Et_2O (1 : 1) mixture resulted in a cloudy maroon colored solution of [Ce(TriNOx)(C≡C-Ph)] (**1-Ce^{Ph}**, see Fig. 2A). The use of 1.6 equiv. Li–C≡C-Ph was based on empirical observation and used to ensure complete formation of the product **1-Ce^{Ph}**. The solvent was stripped under reduced pressure and the resulting solid was washed with Et_2O

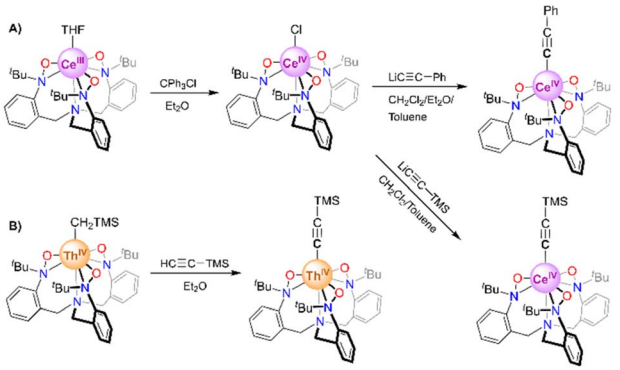

Fig. 2 Syntheses of (A) Ce^{IV}–alkynyl complexes (**1-Ce^{Ph}** and **1-Ce^{TMS}**) and (B) Th^{IV}–alkynyl complex (**1-Th^{TMS}**).

to afford the pure product of **1-Ce^{Ph}** in 80% yield. Maroon X-ray quality crystals were grown from a cooled (−25 °C) solution of **1-Ce^{Ph}** in fluorobenzene with pentane diffusion over 2 days. Complex [Ce(TriNOx)(C≡C-TMS)] (**1-Ce^{TMS}**) was obtained in 64% yield, following a similar procedure where pure toluene was used as the solvent instead of a toluene/Et_2O mixture. Dark maroon X-ray quality crystals of **1-Ce^{TMS}** were grown from a cooled (−25 °C) solution of toluene with pentane diffusion over 3 days. **1-Ce^{TMS}** and **1-Ce^{Ph}** exhibit different solubilities; the former is soluble in Et_2O or toluene and the latter is not. A thorium(IV) analogue was synthesized by addition of a HC≡C-$SiMe_3$ solution in Et_2O to a colorless solution of [Th(CH_2-$SiMe_3$)(TriNOx)] in Et_2O dropwise, resulting in a white cloudy solution (see Fig. 2B). Complex [Th(TriNOx)(C≡C-$SiMe_3$)] (**1-Th^{TMS}**) was obtained in 50% yield following filtration and washing the precipitate with Et_2O. X-ray quality colorless crystals of **1-Th^{TMS}** were similarly grown from a cooled (−25 °C) solution of toluene/dichloromethane with pentane diffusion over 3 days.

X-ray structures of 1-Ce^{Ph}, 1-Ce^{TMS}, and 1-Th^{TMS}

X-ray crystallography experiments confirmed the structures of **1-Ce^{Ph}** and **1-Ce^{TMS}** featuring the –C≡C–R (–R = –Ph or –$SiMe_3$) moiety in the axial position of the $[Ce^{IV}(TriNOx)]^+$ complex. The Ce–C bond distances were 2.501(3) Å for **1-Ce^{Ph}** and 2.513(5) Å for **1-Ce^{TMS}** (Fig. 3). The slightly shorter bond distance in **1-Ce^{Ph}** is consistent with the computational results, *vide infra*.

These Ce^{IV}–C_{sp} bond distances are shorter than the previously reported Ce^{III}–C_{sp} bond distances in cerium–cyanide complexes (2.596(15)–2.736(17) Å),[31] such as $([N^nBu_4]_2[(C_5Me_5)_2Ce^{III}(CN)_3])$; alkynyl complexes (2.549(3)–2.71(2) Å),[32] such as $[(C_5Me_5)_2Ce(CC^tBu)_2Li(THF)]$; and a cerium(III) phenolate alkynyl complex (2.652(9) Å),[33] Na[Ce(CCPh)(bdmmp)$_3$] (bdmmp = 2,6-bis-(dimethylamino)-4-methylphenolate). The shorter distances of the Ce^{IV}–C_{sp} bonds in **1-Ce^{Ph}** and **1-Ce^{TMS}** are consistent with the ∼0.1 Å smaller ionic radius of the cerium(IV) ion compared to cerium(III) with similar coordination numbers.[34] The interatomic distance is summarized into a table (see Table 1 and the SI).

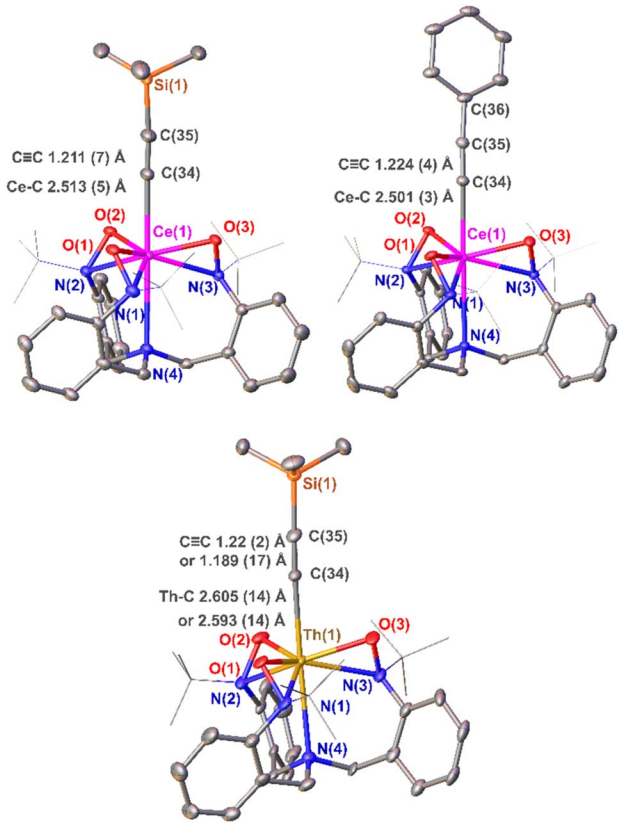

Fig. 3 X-ray crystal structures of **1-Ce^{TMS}**, **1-Ce^{Ph}** and **1-Th^{TMS}**. Thermal ellipsoids were plotted at a 30% probability level. For clarity, hydrogens and solvent molecules in the crystal structure are omitted; *tert*-butyl groups are displayed in wireframe.

These Ce^{IV}–C_{sp} bond distances are also shorter than those of previously reported single Ce^{IV}–C bonds in Ce^{IV} N-heterocyclic carbene complexes (2.652(7)–2.705(2) Å),[25] such as Ce^{IV}[$OCMe_2$-CH_2(1-C{NCHCHN^{i}Pr})]$_4$; Ce^{IV} oxazolide aryl complexes (2.571(7)–2.5806(19) Å),[2] such as [Li(DME)$_3$][Ce^{IV}{κ^2-dihydrodimethyl-2-[4-(trifluoromethyl)phenyl]-oxazolide}]$_3$(2,2′-methylenebis(6-*tert*-butyl-4-methylphenolate)$_2$); Ce^{IV} tris(imidazoline-2-iminato) alkyl complexes (2.515(4) Å) and aryl complexes (2.539(3) Å);[26] Ce^{IV}

Table 1 Cerium–carbon distance (Å), including literature values and present systems

Bond type	Bond distance (Å)	Reference
Ce^{III}–$C_{cyanide}$	2.596(15)–2.736(17)	31
Ce^{III}–$C_{alkynyl}$	2.549(3)–2.71(2)	32
Ce^{III}–$C_{alkynyl}$	2.652(9)	33
Ce^{IV}–$C_{carbene}$	2.652(7)–2.705(2)	25
Ce^{IV}–C_{aryl}	2.571(7)–2.5806(19)	2
Ce^{IV}–C_{aryl}	2.539(3)	26
Ce^{IV}–C_{alkyl}	2.515(4)	26
Ce^{IV}–C_{alkyl}	2.508(2)–2.562(2)	27
Ce^{IV}–$C_{alkynyl}$	2.478(3)–2.523(10)	26
Ce^{IV}–$C_{alkynyl}$	2.513(5)	**1-Ce^{Ph}**
Ce^{IV}–$C_{alkynyl}$	2.501(3)	**1-Ce^{TMS}**
Ce^{IV}–$C_{heter\text{-}atom\ supported\ multiple\ bond}$	2.385(2)–2.441(5)	14

imidophosphorane alkyl complexes (2.508(2)–2.562(2) Å),[27] such as Ce^{IV} benzyl tris(tri-*tert*-butyl imidophosphorane). However, our Ce^{IV}–C_{sp} bond distances are similar to the Ce^{IV}–C bond distances in Ce^{IV} tris(imidazoline-2-iminato) alkynyl complexes (2.478(3)–2.523(10) Å)[26] and are longer than the Ce^{IV} and carbon bond distances in heteroatom-supported bis(iminophosphorano)methandiide complexes (2.385(2)-2.441(5) Å),[14] such as Ce{C[PPh_2-$N(SiMe_3)$]}[O(2,6-diisopropylphenyl)]$_2$ (Fig. 1). The short Ce^{IV}–C_{sp} distances possibly indicate appreciable cerium(IV)–carbon interactions, especially considering that the coordination of the alkynyl moieties to the cerium is unsupported in the case of the compounds reported here.

X-ray crystallography experiments confirmed the molecular structure of related **1-Th^{TMS}** was isostructural to **1-Ce^{TMS}**. There are two independent molecules of **1-Th^{TMS}** in the asymmetric unit with minor differences, with Th–C_{sp} bond distances of 2.593(14) and 2.605 (14) Å. Thorium(IV)–alkynyl complexes were reported previously,[35–39] where the reported Th^{IV}–C bond lengths ranged from 2.450(7) to 2.642(5) Å. The Th^{IV}–C bond distance in **1-Th^{TMS}** is similar to or slightly longer than these literature values, likely due to the electron-donating $TriNOx^{3-}$ ligand. This bond length in **1-Th^{TMS}** is also 0.086 Å longer than the Ce–C distance in **1-Ce^{TMS}**, consistent with a slightly larger ionic radius of thorium(IV) of 1.05 Å than cerium(IV) of 0.97 Å, with an oxidation state of +4 and a coordination number of 8.[34]

NMR spectroscopy and computational studies

Consistent with our previous work,[29] the solution ^{1}H-NMR spectra of the complexes studied here indicated C_{3v} symmetry of the $TriNOx^{3-}$ ligand framework with diastereotopic benzylic protons (CH_2). Complex **1-Ce^{Ph}** exhibits –CH_2 resonances at 4.62–4.59 and 3.08–3.05 ppm and a ^{t}Bu resonance at 0.93 ppm, while **1-Ce^{TMS}** exhibits –CH_2 resonances at 4.57–4.54 and 3.03–3.00 ppm and a ^{t}Bu resonance at 0.97 ppm. The overall chemical shifts were consistent with closed shell complexes for both **1-Ce^{TMS}** and **1-Ce^{Ph}**. Based on the chemical shifts in the ^{1}H-NMR spectra and cerium–carbon bond distances, we assigned **1-Ce^{TMS}** and **1-Ce^{Ph}** as Ce^{IV} complexes.

We also observed previously that the ^{1}H-NMR chemical shifts of the diastereotopic benzylic resonances (CH_2) and *tert*-butyl (^{t}Bu) resonances in the $TriNOx^{3-}$ arms were sensitive to the axial ligand identity. The –CH_2 and –^{t}Bu proton resonances were used to differentiate inner- or outer-sphere coordination to the $[Ce(TriNOx)]^+$ fragment in the solution phase.[29] For example, [Ce(TriNOx)]I exhibits ^{1}H-NMR CH_2 resonances between 4.73–4.67 and 4.07–4.03 ppm and a ^{t}Bu resonance at 0.72 ppm, features that were confirmed to correspond to an outer-sphere iodide anion, whereas the [Ce(TriNOx)Cl] complex has an inner-sphere chloride axial ligand in solution with –CH_2 proton resonances spanning 4.66–4.62 and 3.16–3.12 ppm and characteristic ^{t}Bu resonance at 0.94 ppm. In particular, the larger differences in the diastereotopic –CH_2 chemical shift ranges were correlated with the geometry difference between inner- and outer axial ligand coordination. In the current work, the chemical shifts of **1-Ce^{Ph}** and **1-Ce^{TMS}** resemble those of the inner-sphere [Ce(TriNOx)Cl] at around 3.1 and 0.9 ppm

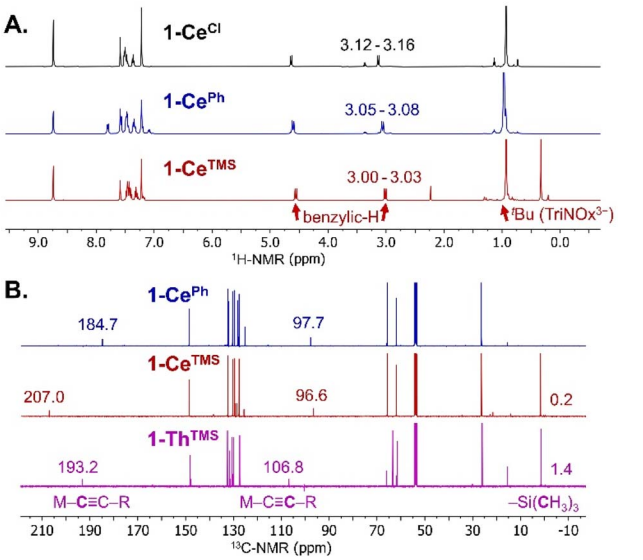

Fig. 4 (A) ^{1}H-NMR spectra of **1-Ce^{Cl}**, **1-Ce^{Ph}** and **1-Ce^{TMS}** recorded in pyridine-d_5. The spectrum of **1-Ce^{TMS}** includes peaks for residual toluene after crystallization and drying. (B) ^{13}C-NMR spectra of **1-Ce^{Ph}**, **1-Ce^{TMS}** and **1-Th^{TMS}** in CD_2Cl_2.

(Fig. 4A). Thus, the chemical shift indicates, as expected, that the alkynyl is coordinated to the cerium(IV) cation in solution, consistent with the result from cyclic voltammetry, *vide infra*. The thorium(IV) alkynyl complex **1-Th^{TMS}** resembles the cerium analogue **1-Ce^{TMS}** in C_6D_6 (see the SI) and was also assigned as an inner-sphere alkynyl complex.

Considering the ^{1}H-NMR resonances of **1-Ce^{Ph}** and **1-Ce^{TMS}** it is noteworthy that the upfield chemical shift of the –CH_2 signals corresponded to a relatively stronger bonding interaction of the axial ligand with the cerium(IV) cation. The trend was noted by us previously for [Ce(TriNOx)Br] (4.71–4.62, 3.34–3.30 ppm), [Ce(TriNOx)Cl] (4.66–4.62, 3.16–3.12 ppm), and [Ce(TriNOx)F] (4.64–4.60, 3.08–3.04 ppm) in pyridine-d_5.[29] In comparison, the –CH_2 ^{1}H-NMR resonances for **1-Ce^{Ph}** (4.62–4.59, 3.08–3.05 ppm) are similar to those for [Ce(TriNOx)F], while the –CH_2 resonance for **1-Ce^{TMS}** (4.57–4.54 and 3.03–3.00 ppm) is further upfield. This result indicates the stronger electron donating ability of –C≡C-$SiMe_3$ than –C≡C-Ph for the Ce^{IV} cation, consistent with the cerium(III/IV) electrochemistry results, the ^{13}C-NMR spectroscopy results, and the observations of a *trans*-influence for the system (*vide infra*).

After confirming the chemical structures and the ^{1}H-NMR spectra of **1-Ce^{TMS}**, **1-Ce^{Ph}** and **1-Th^{TMS}**, we turned to investigations of ^{13}C-NMR spectra. Atoms directly bound to closed-shell heavy metal centers with formally empty d- and/or f-shells, especially actinides, are known to have a characteristic and often large downfield shift.[40,41] This deshielding effect has been correlated with the degree of covalency in the metal–ligand bond.[41–43] The effect has been found, for example, for C_{sp^3}, C_{sp^2} and hydrogen atoms in diamagnetic Th(IV) and U(VI) complexes.[7,44–48] For thorium, the largest ^{13}C-NMR spectroscopy chemical shift δ 230.8 ppm was observed for Th(2-$C_6H_4CH_2$-NMe_2)$_4$,[48] while the largest ^{1}H-NMR chemical shift was

estimated using DFT calculations at 20.3 ppm for ThH $[N(SiMe_3)_2]_3$.[49] Recent progress in obtaining isolable cerium(IV)–carbon bonded complexes has demonstrated similar downfield shifts to those in actinide compounds,[2,3,14,25] where the largest ^{13}C chemical shift of δ 343.5 ppm was observed for a $Ce^{IV}[C(Ph_2PNSiMe_3)_2]_2$ complex.[3] Notably, this cerium(IV) complex had a Ce–C bond supported by heteroatom coordination and conjugation, including two phosphorus atoms bound at the central carbon, qualifying a direct comparison.

In the current cases (Fig. 4B), the ^{13}C chemical shifts are 184.7 ppm for **1-Ce^{Ph}** in CD_2Cl_2 and 207.0 ppm for **1-Ce^{TMS}** in CD_2Cl_2 (and 213.0 ppm in C_6D_6), well outside the typical range for alkynyl resonances (65–90 ppm).[50] Thus, the strong downfield shift indicates potentially a large spin–orbit coupling contribution to the chemical shift, as with other cerium(IV)–carbon moieties.[7] This observation also reflects the strong cerium–alkynyl bonding interactions. [Ce(TriNOx)(**C**≡C-Ph)] has larger ^{13}C-NMR shifts at 184.7 ppm than those reported in the Ce^{IV}–C_{sp} complex $[Ce^{IV}(ImN)_3(\mathbf{C}{\equiv}C\text{-}Ph)]$ at 176.4 ppm by Chen and Li.[26] It should be noted that these ^{13}C-NMR shifts are smaller than those reported in the Ce^{IV}–C_{aryl} complex (255.6 ppm for a cerium oxazolide complex) by us previously.[2] This is presumably because the $^{13}C_{sp^2}$-NMR chemical shift (100–170 ppm for arenes)[2] is intrinsically larger than the $^{13}C_{sp}$-NMR chemical shift (60–100 ppm for alkynes).

To understand the Ce^{IV}/Th^{IV}–C bonding interactions and the influence of spin–orbit coupling, computational analyses were carried out, including calculations of the carbon NMR chemical shifts. Density functional theory (DFT) calculations were initially performed for **1-Ce^{TMS}**, **1-Ce^{Ph}**, and **1-Th^{TMS}** using the B3LYP hybrid functional. Complete computational details are provided in the SI. B3LYP is frequently used for molecular structure optimizations and bonding studies and therefore we used it for these purposes in the present investigation.[51,52] Selected optimized bond distances of **1-Ce^{TMS}**, **1-Ce^{Ph}**, and **1-Th^{TMS}** are compared to the experimental crystal structure data in Table S3. The optimized M–C bond metrics align closely with the experimental data, with deviations of only 0.001 Å and 0.03 Å for the Ce–C and Th–C distances, respectively, confirming the reliability of the chosen computational model.

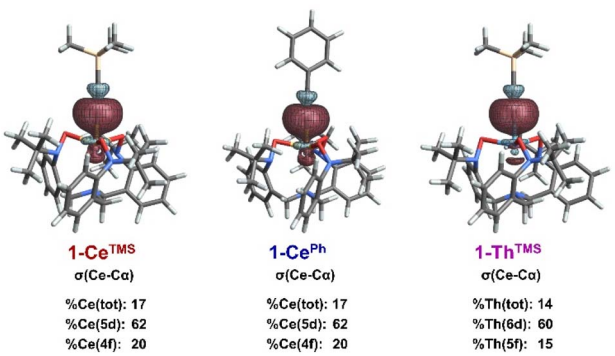

Fig. 5 Isosurfaces (±0.03 a.u.) of σ(Ce–C_α) bonding NLMOs in **1-Ce^{TMS}**, **1-Ce^{Ph}**, and **1-Th^{TMS}**, along with total weight-% metal character and 6d *vs.* 5f contributions at the metal. (Color code: Ce yellow, Th sky blue, Si wheat, C gray, O red, N blue, and H white).

To explore the nature of the M–C interactions, we employed natural localized molecular orbital (NLMO) analyses to assess the covalency resulting from the σ donation in **1-Ce^{TMS}**, **1-Ce^{Ph}**, and **1-Th^{TMS}**. Relevant orbitals are depicted in Fig. 5, and atomic hybrid contributions in the NLMOs and bond order analysis representing the important bonding interactions are listed in Tables S4 and S5. Given the similarity in the bonding characteristic of **1-Ce^{TMS}** and **1-Ce^{Ph}**, we mainly focused on **1-Ce^{TMS}** *versus* **1-Th^{TMS}**. For **1-Ce^{TMS}**, the NLMO analysis reveals a σ(Ce–C_α) bond with 17% total Ce density weight (18% 6s; 62% 5d; 20% 4f), along with two orthogonal π(C_α–C_β) bonds showing negligible Ce weights (1% each). In other words, there is a Ce—C_α σ bond which is polarized toward carbon. The 17% density weight on Ce means that electron density corresponding to about 0.34 electrons is donated to Ce (the NLMO is doubly occupied). In contrast, the σ(Th–C_α) NLMO for **1-Th^{TMS}** exhibits 14% (60% 6d; 15% 5f) Th weight, *i.e.*, lower than that of the Ce analogue. The calculations therefore indicate that the extent of metal–ligand covalent bonding with the ligands studied herein is somewhat more pronounced for Ce(IV)- than for Th(IV)-carbon bonds, which is in line with reported data for thorium(IV)-imido *versus* cerium(IV)-imido complexes from our group.[53] These results and a growing body of evidence suggest that the notion that lanthanide bonding is not covalent is inappropriate.

The ^{13}C-NMR chemical shifts for complexes **1-Ce^{TMS}** and **1-Ce^{Ph}** were calculated using a functional denoted here as PBE0(40) (a PBE-based hybrid with 40% exact exchange), without and with inclusion of the SO interaction. This functional was previously shown to accurately predict ^{13}C-NMR chemical shifts in organometallic cerium complexes.[2,54,55] A summary of calculated shielding constants and chemical shifts is listed in Table S6. The calculated and experimental ^{13}C chemical shifts are in excellent agreement. For example, the calculated C_α shift for **1-Ce^{TMS}** is 207.3 ppm (expt. = 207.0 ppm), which includes a 19.4 ppm deshielding contribution due to SO effects that is primarily attributed to the strong SO coupling within the Ce 4f (and 5d) shell and its involvement in the chemical bond with C_α.

For comparison, the calculated C_α shift for **1-Th^{TMS}** is 195.5 ppm (expt. = 193.2 ppm), with a 25.4 ppm shift due to SO coupling. This is consistent with a weaker covalency of thorium compared with cerium but stronger SO coupling for Th due to the higher nuclear charge. In another comparison, the calculated C_α shift for **1-Ce^{Ph}** is 186.8 ppm (expt. = 184.7 ppm), which includes a 20.4 ppm deshielding from the SO interaction. The similar SOC deshielding in **1-Ce^{Ph}** relative to **1-Ce^{TMS}** is commensurate with its similar Ce–C_α bond covalency.

Vibrational spectroscopy and analysis

Bonding interactions of alkynyl moieties with various cationic moieties were studied by vibrational spectroscopies previously.[56–65] Upon bonding to a metal cation, the metal–alkynyl (M–C) interaction might be expected to influence the vibrational frequency of the –C≡C– moiety due to metal-alkynyl σ- and π-bonding interactions.[56,65] For the present study, we have only considered the impact of σ-bonding interactions.

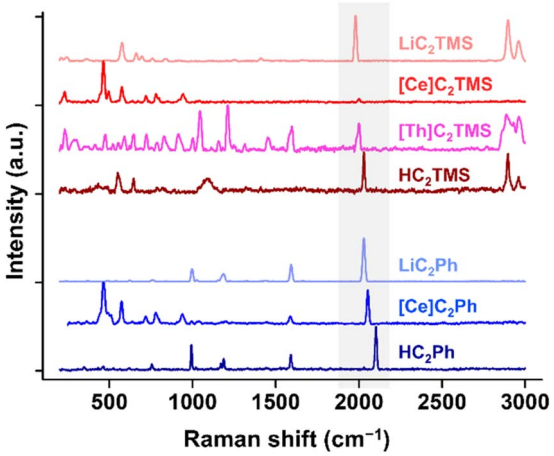

Fig. 6 Raman spectra of 1-Ce^{TMS}, 1-Ce^{Ph}, and 1-Th^{Ph}, and comparison with a lithium–acetylide complex and protonated alkyne.

No vibrational spectra of cerium(IV)–alkynyl complexes have previously been reported. Here, we collected the infrared (IR) absorption and Raman spectra of **1-Ce^{TMS}**, **1-Ce^{Ph}**, and **1-Th^{TMS}** to identify the vibrational frequencies of the –C≡C– moiety (Fig. 6 and the SI) and compared them with those of other metal–alkynyl complexes. For the M–C≡C-TMS complexes, the observed $\nu_{C\equiv C}$ Raman stretching frequencies were 2000 and 2003 cm^{-1} for **1-Ce^{TMS}** and **1-Th^{TMS}** respectively. The notably weak Raman signal for **1-Ce^{TMS}** was intrinsic and observed over multiple samples/measurements. The reasons for the lower Raman signal strength for **1-Ce^{TMS}** compared to **1-Th^{TMS}** are, as yet, unclear. For M–C≡CPh, **1-Ce^{Ph}** (Raman = 2052 cm^{-1}) was shown to have a $\nu_{C\equiv C}$ stretching frequency that was lower than that in HC≡CPh (IR = 2105 cm^{-1} and Raman = 2104 cm^{-1}). Vibrational spectra of related metal–acetylide complexes reported in the literature include Yb(C≡CPh)(C$_5$H$_5$)$_2$ (IR = 2040 cm^{-1})[63] and Zr(C≡CPh)$_2$(C$_5$Me$_5$)$_2$ (IR = 2073 cm^{-1}).[57] Based on these reported results, the vibrational frequency of the alkynyl moiety reflects the metal–alkynyl σ-bond interactions (Fig. S48). We contend that the $\nu_{C\equiv C}$ stretching frequencies for **1-Ce^{TMS}**, **1-Ce^{Ph}**, and **1-Th^{TMS}** are approximately intermediate between those observed for more purely ionic f-block (low frequency) and relatively more covalent d-block (high frequency) metal congeners.[1,16,21]

Magnetometry, L_3-edge X-ray absorption spectroscopy and UV-vis absorption spectroscopy

The short Ce–C bonds, downfield ^{13}C chemical shifts, negative reduction potentials and characteristic $\nu_{C\equiv C}$ stretching frequencies highlighted the interactions between cerium metal and alkynyl ligands in **1-Ce^{TMS}** and **1-Ce^{Ph}**. These complexes present an opportunity for further study, as the unfilled low-lying 4f-orbitals in cerium(IV) can result in multi-configurational ground states in some cases.[6,66]

The Ce L_3-edge (Ce 2p → 5d) X-ray absorption near edge structure (XANES) spectra of **1-Ce^{TMS}** and **1-Ce^{Ph}** are shown in Fig. S56–S57. A characteristic double-peaked structure is observed, which is attributed to excitations of the core hole electron (2p) to 4f$^1\bar{L}$5d^1 and 4f^{0}5d^1 final states, where $\bar{L}$ indicates a hole (vacancy) at the ligand.[6,17] The intensities of both peaks were evaluated using established curve-fitting methods, which indicated that the weight of the 4f^{0}5d^1 configuration had statistically equivalent values for both complexes, with relative weights of 0.43(3) for **1-Ce^{TMS}** and 0.46(3) for **1-Ce^{Ph}**. These configuration weights are comparable to those of other cerium(IV) complexes, such as cerium(IV) TriNOx^{3-} imido complexes (0.37(3)–0.45(3))[6] and cerium(IV) TriNOx^{3-} oxo complexes (0.39(3)–0.41(3)).[6] Although fitting was unable to quantify any difference, visual inspection of the normalized spectra shows that the feature at higher energy is more intense for **1-Ce^{Ph}**. We reach the qualitative determination that the 4f electron density at Ce is lower for **1-Ce^{Ph}** relative to **1-Ce^{TMS}**.

Having evaluated the amount of charge transfer for **1-Ce^{TMS}** and **1-Ce^{Ph}**, we next turned to temperature dependent magnetic studies of the compounds. Van Vleck temperature-independent paramagnetism (TIP) has been observed for molecules, formally cerium(IV) complexes,[6,66–68] arising from small energy differences between the open-shell singlet ground state and admixed, low-lying triplet excited states.[67] Magnetometry studies were carried out on **1-Ce^{Ph}**. The variable field magnetization was collected for **1-Ce^{Ph}** at 2 K, which shows the presence of a negligible magnetic impurity that saturates below $M < 0.01$ μB (Fig. S52), indicating the +IV oxidation state of cerium in **1-Ce^{Ph}**. A variable temperature magnetic susceptibility plot for **1-Ce^{Ph}** was collected at a 1.0T applied field (Fig. S53 and S54). The susceptibility plot of χT *vs.* T shows a linear decrease from high (300 K) to low temperature (2 K). After accounting for the intrinsic diamagnetic contribution using Pascal's constants, the TIP value for this cerium(IV) complex was determined to be 6.34(1) × 10^{-4} emu mol^{-1}. This value is similar to, or larger than, those of reported cerium(IV) complexes such as cerocene (1.4(2) × 10^{-4} emu mol^{-1}),[68] [NEt$_4$]$_2$[CeCl$_6$] (1.6(2) × 10^{-4} emu mol^{-1}),[66] and [K(DME)$_2$][Ce(TriNOx)(=NAr^F)] (2.2(2) × 10^{-4} emu mol^{-1}).[6] UV-vis absorption spectra were recorded for both **1-Ce^{TMS}** and **1-Ce^{Ph}**, where **1-Ce^{TMS}** showed a peak at 358 nm and **1-Ce^{Ph}** showed a peak at 382 nm, and both were attributed to LMCT (Fig. S50). Overall, our experimental data confirm pure cerium(IV) oxidation states and reveal the electronic structure and configuration for the cerium–alkynyl complex.

Electrochemical studies

To better understand the impact of the alkynyl group on the stabilization of the cerium(IV) ion, electrochemical studies were performed on **1-Ce^{Ph}** and **1-Ce^{TMS}** to measure the potential of the Ce(III/IV) redox couple. The electrochemical properties of [Ce^{IV}(TriNOx)X] were studied previously to identify the solution speciation and compare the redox potentials, where X$^-$ = F$^-$, Cl$^-$, Br$^-$, I$^-$, OTf$^-$ (OTf$^-$ = CF$_3$SO$_2$O$^-$), or [NAr^F][M(L)$_x$]$^-$ (Ar^F = 3,5-(CF$_3$)$_2$-C$_6$H$_3$; M = Li, K, Rb, or Cs; L = THF, TMEDA, DME, or 2.2.2-cryptand, x = 1 or 2). The previously reported redox potentials of the [Ce^{IV}(TriNOx)]$^+$ framework were in accord with the electron-donating character of the axially coordinated moieties. For example, the potentials of the reduction waves

versus Fc/Fc$^+$ of the Ce(IV) compounds with axial ligands ranging from weakly donating to strongly donating ligands are [Ce(TriNOx)][OTf] ($E_{pc} = -1.04$ V), [Ce(TriNOx)Br] ($E_{pc} = -1.04/-1.16$ V), [Ce(TriNOx)Cl] ($E_{pc} = -1.26$ V), [Ce(TriNOx)F] ($E_{pc} = -1.40$ V) and [M(L)$_x$][Ce(TriNOx) = N–Ar] (–Ar = –(3,5-(CF$_3$)$_2$C$_6$H$_3$), $E_{pc} = -1.39$ to -1.45 V) at a 100 mV s^{-1} scan rate (Fig. 7).[69] We performed cyclic voltammetry studies of **1-Ce^{TMS}** and **1-Ce^{Ph}** under similar conditions (Fig. 7A). Reduction features were observed for **1-Ce^{TMS}** at $E_{pc} = -1.66$ V *vs.* Fc/Fc$^+$ and **1-Ce^{Ph}** at $E_{pc} = -1.58$ V. The E_{pc} values compared with that of [Ce(TriNOx)][OTf] ($E_{pc} = -1.04$ V) with an outer-sphere OTf$^-$ ligand indicate inner-sphere coordination of the cerium alkynyl in solution in both cases.

The relatively negative E_{pc} values of the cerium(IV) alkynyl complexes indicate the strong electron donating character of the alkynyl ligand, notably stronger than that of the fluoride ligand, with a ~0.2 V more negative redox potential. It should be noted that although the cerium(IV) imido complexes have a E_{pc} values less negative than that of the alkynyl analogues: [M(L)$_x$][Ce(TriNOx) = N–Ar] (–Ar = –(3,5-(CF$_3$)$_2$C$_6$H$_3$), $E_{pc} = -1.39$ to -1.45 V), this observation is likely due to the reduction of the imido ligand instead of a cerium(IV) cation. Indeed, the imido ligand is a better electron-donating ligand, as indicated in the *trans*-influence section, *vide infra*. In comparison, they have a similar reduction potential to [Li(THF)$_4$][Ce(κ^2-*ortho*-oxa)(MBP)$_2$],[26] while [Ce^{IV}(Alkyl)(NP(*tert*-butyl)$_3$)$_3$] has a much more negative reduction potential (-2.55 V to -2.92 V) due to the strong electron donating –N=P(*tert*-butyl) moiety in addition to an alkyl ligand.[27] In general, these electrochemical data provide supporting evidence for a strong interaction between the Ce(IV) cation and –C≡C–R moieties (–R = –SiMe$_3$ or –Ph).

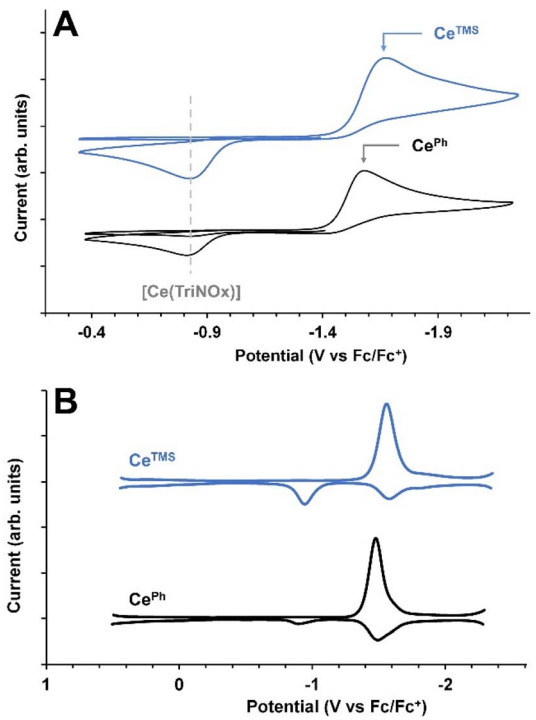

Fig. 7 (A) Cyclic voltammograms (CVs) of **1-Ce^{TMS}** and **1-Ce^{Ph}** (3 mM) in CH_2Cl_2 using [^{n}Pr$_4$N][BAr$^F_4$] (100 mM) as the supporting electrolyte. Scan rate: 100 mV s^{-1}. All sweeps were performed in the oxidative direction. The trace shows reduction features for **1-Ce^{TMS}** ($E_{pc} = -1.66$ V) and **1-Ce^{Ph}** ($E_{pc} = -1.58$ V), followed by an oxidation feature at $E_{pa} = -0.82/-0.81$ V, the latter of which does not appear in the first scan. (B) Differential Pulse Voltammagrams (DPVs) of **1-Ce^{TMS}** and **1-Ce^{Ph}**.

Table 2 Cerium (III/IV) redox potential. [Ce^{IV}(TriNOx)]$^+$ derivatives, several common Ce^{IV} complexes, and several Ce^{IV}–C complexes from the literature are shown for comparison

Complex	E_{pc}	$E_{1/2}$
[Ce(TriNOx)](OTf)	−1.04 V	−0.95 V
[Ce(TriNOx)]I	−1.04 V	—
[Ce(TriNOx)Br]	−1.16 V (−1.04 V)	—
[Ce(TriNOx)Cl]	−1.26 V	—
[Ce(TriNOx)F]	−1.40 V	−1.36 V
[M][Ce(TriNOx)=NAr]	−1.39 V to −1.45 V	—
[Ce(TriNOx)(C≡CPh)]	**−1.58 V**	**−1.49 V (E_p)**[a]
[Ce(TriNOx)(C≡CTMS)]	**−1.66 V**	**−1.57 V (E_p)**[a]
[N^{n}Bu$_4$]$_2$[Ce(NO$_3$)$_6$]	—	0.62 V
[CeCl$_6$]$^{2-}$	—	0.03 V
[Ce[N(SiMe$_3$)$_2$]$_3$Cl]	—	−0.30 V
[Ce(COT)$_2$]	—	−1.40 V
[Ce(BIPM^{TMS})$_2$]	—	−1.63 V
[Li(THF)$_4$][Ce(κ^2-*ortho*-oxa)(MBP)$_2$]	−1.67 V	—
[Ce^{IV}(Alkyl)(NP(*tert*-butyl)$_3$)$_3$]	[b]−2.55 V to −2.92 V	—

[a] E_p stands for redox potential from differential pulse voltammetry (DPV) instead of $E_{1/2}$. [b] The scan rate was unknown, while other E_{pc} values were measured at a 100 mV s^{-1} scan rate.

Reduction waves (E_{pc}) for **1-Ce^{TMS}** and **1-Ce^{Ph}** demonstrate the reduction of the Ce(IV) alkynyl complexes to corresponding Ce(III) moieties (Fig. 7A and Table 2). However, this process is largely irreversible due to an accompanying chemical process. In this process, the reduced species, [Ce^{III}(C≡C–R)(TriNOx)]$^-$, is not stable and the alkynyl ligand presumably dissociates under the electrochemical conditions employed, similar to reported results for [Ce^{III}Cl(TriNOx)]$^-$.[29] Following the cathodic features of **1-Ce^{TMS}** and **1-Ce^{Ph}**, the subsequent anodic sweeps (E_{pa}) indicate the oxidation of the newly generated Ce(III) species, likely "[Ce^{III}(TriNOx)]", based on the observed oxidation potential and comparison with our previous results.[29]

Differential pulse voltammetry (DPV) experiments[70] were also used to determine potential values for the redox processes of **1-Ce^{TMS}** and **1-Ce^{Ph}**, where $E_p = -1.57$ V for **1-Ce^{TMS}** and -1.49 V for **1-Ce^{Ph}** *vs.* Fc/Fc$^+$ (Fig. 7B), for comparison with the measured $E_{1/2}$ values (Table 2).[29,71] These observed E_p values are more negative than those of some commonly observed cerium(IV) complexes and are comparable with those of other organo-cerium(IV) complexes such as [Ce(COT)$_2$] or [Ce^{IV}(BIPM^{TMS})$_2$].[2,3,14]

Observation of a *trans*-influence in the [Ce^{IV}X(TriNOx)] series

The *trans*-influence is a structural phenomenon where a ligand bonded to a metal center weakens the bond of the metal to a second ligand located in the *trans* position. The structural *trans*-influence is well established for transition metal complexes,[72,73] especially for heavy, late transition metals. Some

Table 3 Data relevant to computational studies on *trans*-influence. The data include Ce–N(4) computed distance, Ce–X and Ce–N(4) Mayer bond orders, and LUMO energy

	Computed distance (Å)	Bond order		Energy
Axial ligand X to $[Ce(TriNOx)]^+$	Ce–N(4)	Ce–X	Ce–N(4)	E_{LUMO} (Hartree)
THF	2.826	0.2564	0.2590	−0.1884
I^-	3.082	0.7353	0.1821	−0.0873
Br^-	3.111	0.9373	0.1712	−0.0820
Cl^-	3.129	0.9726	0.1695	−0.0821
F^-	3.147	1.0430	0.1559	−0.0767
$^-C{\equiv}C$-Ph	3.082	0.8552	0.1660	−0.0710
$^-C{\equiv}C$-TMS	3.069	0.8506	0.1691	−0.0772
$^-$NHAr	3.071	0.7999	0.1711	−0.0831
$^-OSiPh_3$	3.187	0.8972	0.1485	−0.0758
=NAr Li(TMEDA)	3.228	1.1970	0.1359	−0.0520
=NAr $K(DME)_2$	3.335	1.5158	0.1151	−0.0383
=NAr [Cs(Cryptand)]	3.510	1.7020	0.0774	0.0550

reports, typically structural ones, were also presented on the *trans*-influence in lanthanide(III) complexes.[74–77] Conversely, the inverse-*trans*-influence has been described in high oxidation state actinide complexes,[3,42,43,78–83] where a ligand in a complex strengthens, rather than weakens, the bond of the ligand *trans* to it. Our group has studied this phenomenon in uranium(V, VI) chemistry previously.[42,43,81] However, there are open questions on the appearance of a *trans*-influence or inverse-*trans*-influence in cerium(IV) complexes, where few studies have been conducted. The Liddle group discussed the possibility of an inverse-*trans*-influence in the tetravalent cerium(IV) phosphoimido complexes,[3] but the influence(s) at cerium(IV) requires additional study with a broad series of compounds (Table 3).

In the current work, a *trans*-position has been studied for the current and previously reported, structurally conserved [Ce^{IV}(-TriNOx)X] complexes, considering the axial nitrogen atom N(4) from the tridentate $TriNOx^{3-}$ ligand and terminal X^- (or L) ligand (Fig. 8). For example, X^- in **1-Ce^{TMS}**/**1-Ce^{Ph}** indicates the alkynyl ligands. The angles of X–Ce–N(4)$_{TriNOx}$ of the complexes range from 173.8(3)° to 179.34(8)° in the crystal structures and range from 172.84° to 179.98° in the DFT optimized structures, indicating the validity for the *trans*-position of X^- and N(4) atoms on the cerium atom. A series of X^- (or L) ligands for the complexes have been compared from weakly coordinating to strongly coordinating: -THF, -halide (iodide, bromide, chloride, and fluoride), -alkynyl, -anilide, -siloxide, and -imide (Li-capped,

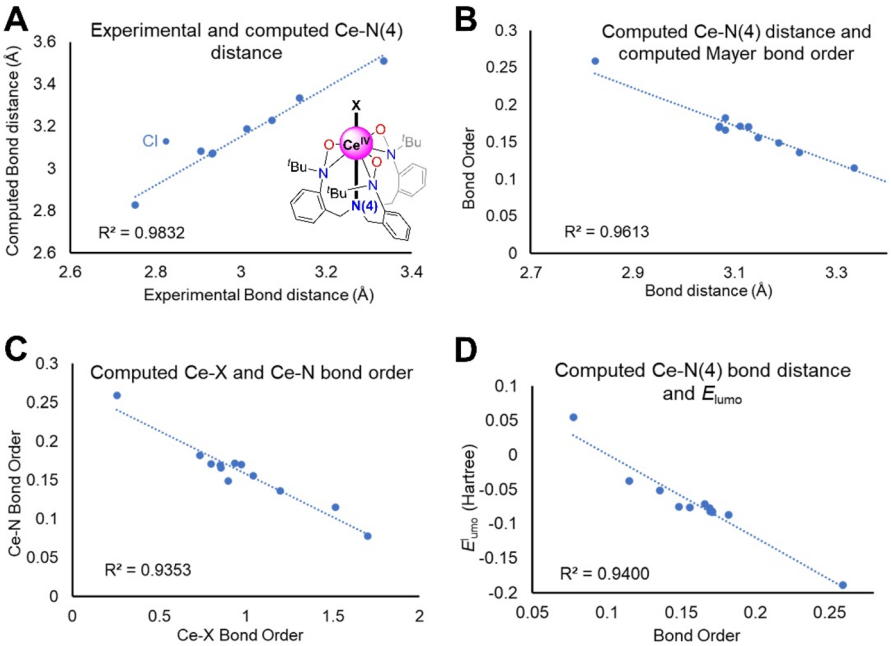

Fig. 8 *Trans*-influence on [Ce(TriNOx)(X)] complexes. (A) Experimental and computed Ce–N(4) distance (Cl was excluded as an outlier). (B) Computed Ce–N(4) distance and Mayer bond order. (C) Computed Ce–X bond order and Ce–N(4) bond order. (D) Computed Ce–N(4) bond distance and LUMO energy correlation.

K-capped and uncapped imides) (see the SI). The Ce(IV)–N(4) bonding interaction is understood to be weak but nevertheless an important and diagnostic metric on axial bonding in this system. It should be noted that, in the solution phase, the iodide ligand is an outer-sphere and bromide ligand is partially outer-sphere (in chemical equilibrium between the inner- and outer-sphere). But these two ligands, I^- and Br^-, were considered inner spheres for the structures considered in this study. The complexes were ranked by increasing Ce–N(4) distance, excepting the halides. Among halide complexes [Ce^{IV}(TriNOx)X, X = F^-, Cl^-, Br^-, I^-], only the Cl^- complex was previously characterized by crystallography, while the rest were characterized by elemental analysis and NMR.[29] Here, all the halide complexes were used as model complexes for computational studies. It should also be noted that these computational studies on the *trans*-influence used methods, with the B3LYP hybrid functional, that were chosen for consistency with previous work on the [Ce^{IV}(TriNOx)X] system.[29]

We posited that the most telling case for the *trans* influence in the current system would be made with multiple lines of experimental and computational metrics that incorporate X-ray structural and computational electronic structural aspects concurrently (Fig. 8).[43] The computational methods undertaken here are different from those described in previous sections of the current work and a description of the *trans* influence computational study is also provided in the SI. As described before,[29] the accuracy between the computed distance of Ce–O_{TriNOx} and experimental result indicates an acceptable computational model performance. The Ce–X distances exhibit a good correlation between the experimental and computed results, with differences less than 0.08 Å, except for the chloride complex (0.12 Å). The Ce–$N(4)_{TriNOx}$ distances also demonstrated reasonable agreement between experimental and computed values, except for chloride (Fig. 8A). We also observed a negative correlation between computed Ce–N(4) bond distance and Mayer bond order (Fig. 8B), consistent with a stronger bond with a shorter distance.

Mayer bond order has been used to compare the halide derivatives of [Ce^{IV}(TriNOx)X] complexes.[29] Based on the computational results in Fig. 8C, it is evident that a larger Mayer bond order of Ce–X (or L) exhibits a *trans*-influence and results in a smaller Mayer bond order of Ce^{IV}–N(4), indicating the stronger donating ability of the X/L ligand on cerium resulting in a weaker bond between Ce and N(4). The LUMO of these complexes primarily consists of 4f character and the LUMO energies are correlated with the electron donating ability of the ligands.[84] We observe a similar trend between the LUMO energy and Ce–N(4) distance, where a stronger Ce–X bond and longer but weaker Ce–N(4) bond result in a higher LUMO energy (Fig. 8D), similar to previous observation.[29]

To better illustrate the *trans*-influence, this phenomenon can be interpreted using the Ce–N(4) experimental bond distances (Table S1). Weakly coordinated THF resulted in a Ce–N(4) bond length of 2.717(9)–2.787(8) Å and the chloride (Cl^-) ligand resulted in a Ce–N(4) bond length of 2.825(3) Å. The relatively strong sigma-donating alkynyl ligands yielded a Ce–N(4) bond length of 2.906(2) Å for [Ce(TriNOx)(C≡C-Ph)] and 2.932 Å for [Ce(TriNOx)(C≡C-TMS)], whereas the anilide ligand resulted in a bond length of 2.934(3) Å for [Ce(TriNOx)(NHAr)] (Ar = (3,5-$(CF_3)_2C_6H_3$)). Thus, notably, the alkynyl ligand exhibits a strong donating ability comparable to that of the anilide ligand, indicating a stronger bonding interaction between cerium and alkynyl moieties (see the SI). By way of comparison, the extraordinarily strongly coordinating uncapped imido ligand gives a bond distance of 3.335 Å for Ce–N(4) of [Cs(2,2,2-crypt-and)][Ce(TriNOx)(NAr)]. To conclude, the bond distance and bond order well reflect the bonding interactions of the Ce–X and Ce–N(4) moieties and illustrate a structural *trans*-influence is operative in this series.

Conclusions and outlook

The synthesis and characterization of cerium(IV)/thorium(IV) alkynyl complexes, **1-Ce^{Ph}**, **1-Ce^{TMS}**, and **1-Th^{TMS}**, have expanded the understanding of cerium/throium-carbon bonding by providing insights into their structural, spectroscopic, and electrochemical properties. These studies reveal the unique covalent contributions of Ce 5d- and 4f-orbitals in M–C bonding interactions, as evidenced by X-ray crystallography, Raman spectroscopy, and ^{13}C-NMR spectroscopy chemical shifts. Comparative analyses with thorium(IV) analogues and other cerium(IV) complexes highlight the strong electron-donating nature of alkynyl ligands, resulting in notable redox properties. Furthermore, these findings challenge traditional notions of f-element bonding, by emphasizing the significant covalency in Ce(IV)–carbon bonds and the influence of spin–orbit coupling effects. The observed *trans*-influence in the [Ce^{IV}(TriNOx)X] framework enriches our understanding of ligand-field effects in high oxidation state lanthanide complexes and offers a foundation for future studies on bonding and possibly unique reactivity in f-block chemistry.

Author contributions

Q. Y. proposed and synthesized **1-Ce^{TMS}** and **1-Ce^{Ph}**, conducted NMR spectroscopy, electrochemistry, UV-vis spectroscopy, and *trans*-influence studies and drafted an initial manuscript draft. Q. Y. and E. L. synthesized **1-Th^{TMS}**. X. Y. and J. A. conducted the computational analysis for **1-Ce^{TMS}**, **1-Ce^{Ph}** and **1-Th^{TMS}**. The *trans*-influence computational study was carried out by Q. Y. with input from X. Y. and J. A. aspects of the work. P. P. and Q. Y. conducted the Raman and IR studies. P. P. conducted elemental analysis of the three complexes reported. P. W. S. and S. G. M. conducted the XAS studies. H. G. conducted the magnetism studies with Q. Y. taking part. Q. Y., E. L., X. Y., J. A. and E. J. S. wrote the manuscript. All co-authors participated in the revisions. M. R. G. and P. J. C. resolved the crystal structures. E. J. S. supervised all aspects of the project.

Conflicts of interest

There are no conflicts to declare.

Data availability

The data supporting this article have been included as part of the SI. Crystallographic data for **1-Ce^{TMS}**, **1-Ce^{Ph}** and **1-Th^{TMS}** have been deposited at the CCDC under 2448118–2448120 and can be obtained from **https://www.ccdc.cam.ac.uk/structures/**.

CCDC 2448118–2448120 contain the supplementary crystallographic data for this paper.[85–87]

The supplementary information includes NMR spectroscopic, X-ray crystallographic, electrochemical, vibrational spectroscopic, UV-vis spectroscopic, magnetometric, X-ray absorption spectroscopic, and computational data. See DOI: **https://doi.org/10.1039/d5sc03222a**.

Acknowledgements

Q. Y. thanks Dr Bren E. Cole for his mentorship, support and assistance on [Ce(TriNOx)Cl] synthesis. E. J. S. thanks the U. S. National Science Foundation (CHE-2247668) for financial support of this work. E. J. S. also thanks the University of Pennsylvania for support. This work was supported at Lawrence Berkeley National Laboratory by the Director, Office of Science, Office of Basic Energy Sciences, Division of Chemical Sciences, Geosciences, and Biosciences Heavy Element Chemistry (HEC) program of the United States Department of Energy (DOE) under contract DE-AC02-05CH11231. We also thank JASCO for use of Raman instrumentation in the JASCO facility for Spectroscopic Excellence in the Chemistry Department at the University of Pennsylvania. X. Y. and J. A. thank the center for computational research at U. Buffalo (**https://hdl.handle.net/10477/79221**) for providing computational resources.

Notes and references

1 M. L. Neidig, D. L. Clark and R. L. Martin, Covalency in f-element complexes, *Coord. Chem. Rev.*, 2013, **257**(2), 394–406.

2 G. B. Panetti, D.-C. Sergentu, M. R. Gau, P. J. Carroll, J. Autschbach, P. J. Walsh and E. J. Schelter, Isolation and characterization of a covalent CeIV-Aryl complex with an anomalous 13C chemical shift, *Nat. Commun.*, 2021, **12**(1), 1713, DOI: **10.1038/s41467-021-21766-4**.

3 M. Gregson, E. Lu, D. P. Mills, F. Tuna, E. J. L. McInnes, C. Hennig, A. C. Scheinost, J. McMaster, W. Lewis, A. J. Blake, *et al.*, The inverse-trans-influence in tetravalent lanthanide and actinide bis(carbene) complexes, *Nat. Commun.*, 2017, **8**(1), 14137, DOI: **10.1038/ncomms14137**.

4 T. Cheisson and E. J. Schelter, Rare earth elements: Mendeleev's bane, modern marvels, *Science*, 2019, **363**(6426), 489–493, DOI: **10.1126/science.aau7628**.

5 P. Pandey, Q. Yang, M. R. Gau and E. J. Schelter, Evaluating the photophysical and photochemical characteristics of green-emitting cerium(iii) mono-cyclooctatetraenide complexes, *Dalton Trans.*, 2023, **52**(18), 5909–5917, DOI: **10.1039/D3DT00351E**.

6 L. M. Moreau, E. Lapsheva, J. I. Amaro-Estrada, M. R. Gau, P. J. Carroll, B. C. Manor, Y. Qiao, Q. Yang, W. W. Lukens, D. Sokaras, *et al.*, Electronic structure studies reveal 4f/5d mixing and its effect on bonding characteristics in Ce-imido and -oxo complexes, *Chem. Sci.*, 2022, **13**(6), 1759–1773, DOI: **10.1039/D1SC06623D**.

7 J. Autschbach, The role of the exchange-correlation response kernel and scaling corrections in relativistic density functional nuclear magnetic shielding calculations with the zeroth-order regular approximation, *Mol. Phys.*, 2013, **111**(16–17), 2544–2554, DOI: **10.1080/00268976.2013.796415**.

8 J. W. Gilge and H. W. Roesky, Structurally Characterized Organometallic Hydroxo Complexes of the f- and d-Block Metals, *Chem. Rev.*, 1994, **94**(4), 895–910, DOI: **10.1021/cr00028a003**.

9 Q. Yang, Y.-H. Wang, Y. Qiao, M. Gau, P. J. Carroll, P. J. Walsh and E. J. Schelter, Photocatalytic C-H activation and the subtle role of chlorine radical complexation in reactivity, *Science*, 2021, **372**(6544), 847–852, DOI: **10.1126/science.abd8408**.

10 Q. Yang, E. Song, Y. Wu, C. Li, M. R. Gau, J. M. Anna, E. J. Schelter and P. J. Walsh, Mechanistic Investigation of the Ce(III) Chloride Photoredox Catalysis System: Understanding the Role of Alcohols as Additives, *J. Am. Chem. Soc.*, 2025, **147**(2), 2061–2076, DOI: **10.1021/jacs.4c15627**.

11 E. Lapsheva, Q. Yang, T. Cheisson, P. Pandey, P. J. Carroll, M. Gau and E. J. Schelter, Electronic Structure Studies and Photophysics of Luminescent Th(IV) Anilido and Imido Complexes, *Inorg. Chem.*, 2023, **62**(15), 6155–6168, DOI: **10.1021/acs.inorgchem.3c00375**.

12 L. A. Solola, A. V. Zabula, W. L. Dorfner, B. C. Manor, P. J. Carroll and E. J. Schelter, An Alkali Metal-Capped Cerium(IV) Imido Complex, *J. Am. Chem. Soc.*, 2016, **138**(22), 6928–6931, DOI: **10.1021/jacs.6b03293**.

13 L. A. Solola, A. V. Zabula, W. L. Dorfner, B. C. Manor, P. J. Carroll and E. J. Schelter, Cerium (IV) imido complexes: structural, computational, and reactivity studies, *J. Am. Chem. Soc.*, 2017, **139**(6), 2435–2442.

14 M. Gregson, E. Lu, J. McMaster, W. Lewis, A. J. Blake and S. T. Liddle, A Cerium(IV)–Carbon Multiple Bond, *Angew. Chem., Int. Ed.*, 2013, **52**(49), 13016–13019, DOI: **10.1002/anie.201306984**.

15 M. D. Walter, C. H. Booth, W. W. Lukens and R. A. Andersen, Cerocene Revisited: The Electronic Structure of and Interconversion Between Ce2(C8H8)3 and Ce(C8H8)2, *Organometallics*, 2009, **28**(3), 698–707, DOI: **10.1021/om7012327**.

16 G. R. Choppin, Covalency in f-element bonds, *J. Alloys Compd.*, 2002, **344**(1–2), 55–59.

17 Q. Yang, Y. Qiao, A. McSkimming, L. M. Moreau, T. Cheisson, C. H. Booth, E. Lapsheva, P. J. Carroll and E. J. Schelter, A hydrolytically stable Ce(iv) complex of glutarimide-dioxime, *Inorg. Chem. Front.*, 2021, **8**(4), 934–939, DOI: **10.1039/D0QI00969E**.

18 Q. Yang, *Organometallic and Photochemistry of Cerium and Thorium Complexes and Photocatalytic Systems for the Generation of Chlorine Radicals*, University of Pennsylvania, 2022.

19 W. J. Evans, T. J. Deming and J. W. Ziller, The utility of ceric ammonium nitrate-derived alkoxide complexes in the synthesis of organometallic cerium(IV) complexes. Synthesis and first x-ray crystallographic determination of a tetravalent cerium cyclopentadienide complex, (C5H5) 3Ce(OCMe3), *Organometallics*, 1989, **8**(6), 1581–1583, DOI: 10.1021/om00108a042.

20 P. Dröse, A. R. Crozier, S. Lashkari, J. Gottfriedsen, S. Blaurock, C. G. Hrib, C. Maichle-Mössmer, C. Schädle, R. Anwander and F. T. Edelmann, Facile Access to Tetravalent Cerium Compounds: One-Electron Oxidation Using Iodine(III) Reagents, *J. Am. Chem. Soc.*, 2010, **132**(40), 14046–14047, DOI: 10.1021/ja107494h.

21 A. Kerridge, Oxidation state and covalency in f-element metallocenes (M = Ce, Th, Pu): a combined CASSCF and topological study, *Dalton Trans.*, 2013, **42**(46), 16428–16436, DOI: 10.1039/C3DT52279B.

22 A. Streitwieser, S. A. Kinsley, C. H. Jenson and J. T. Rigsbee, Synthesis and Properties of Di-π-[8]annulenecerium(IV), Cerocene, *Organometallics*, 2004, **23**(22), 5169–5175, DOI: 10.1021/om049743+.

23 A. Greco, S. Cesca and W. Bertolini, New 7r-cyclooctate'I'raenyl and iT-cyclopentadienyl complexes of cerium, *J. Organomet. Chem.*, 1976, **113**(4), 321–330, DOI: 10.1016/S0022-328X(00)96143-6.

24 G. Balazs, F. G. N. Cloke, J. C. Green, R. M. Harker, A. Harrison, P. B. Hitchcock, C. N. Jardine and R. Walton, Cerium(III) and Cerium(IV) Bis(η8-pentalene) Sandwich Complexes: Synthetic, Structural, Spectroscopic, and Theoretical Studies, *Organometallics*, 2007, **26**(13), 3111–3119, DOI: 10.1021/om7002738.

25 I. J. Casely, S. T. Liddle, A. J. Blake, C. Wilson and P. L. Arnold, Tetravalent cerium carbene complexes, *Chem. Commun.*, 2007, (47), 5037–5039, DOI: 10.1039/B713041D.

26 B. Feng, L.-W. Ye, N. Wang, H.-S. Hu, J. Li, M. Tamm and Y. Chen, Endeavoring Cerium (IV)-Alkyl,-Aryl and-Alkynyl Complexes by an Energy-Level Match Strategy, *CCS Chem.*, 2025, **7**(4), 1043–1053, DOI: 10.31635/ccschem.024.202404131.

27 H. Tateyama, A. C. Boggiano, C. Liao, K. S. Otte, X. Li and H. S. La Pierre, Tetravalent Cerium Alkyl and Benzyl Complexes, *J. Am. Chem. Soc.*, 2024, **146**(15), 10268–10273.

28 B. D. Vincenzini, X. Yu, S. Paloc, P. W. Smith, H. Gupta, P. Pandey, G. T. Kent, O. Ordonez, T. Keller, M. R. Gau, *et al.*, 4f-orbital covalency enables a single-crystal-to-single-crystal ring-opening isomerization in a CeIV–cyclopropenyl complex, *Nat. Chem.*, 2025, **17**, 961–967, DOI: 10.1038/s41557-025-01791-2.

29 J. A. Bogart, C. A. Lippincott, P. J. Carroll, C. H. Booth and E. J. Schelter, Controlled Redox Chemistry at Cerium within a Tripodal Nitroxide Ligand Framework, *Chem.–Eur. J.*, 2015, **21**(49), 17850–17859, DOI: 10.1002/chem.201502952.

30 E. N. Lapsheva, T. Cheisson, C. Álvarez Lamsfus, P. J. Carroll, M. R. Gau, L. Maron and E. J. Schelter, Reactivity of Ce(iv) imido compounds with heteroallenes, *Chem. Commun.*, 2020, **56**(35), 4781–4784, DOI: 10.1039/C9CC10052K.

31 J. Maynadié, J.-C. Berthet, P. Thuéry and M. Ephritikhine, Cyanide metallocenes of trivalent f-elements, *Organometallics*, 2007, **26**(10), 2623–2629.

32 D. Schneider and R. Anwander, Pentamethylcyclopentadienyl-Supported Cerocene(III) Complexes, *Eur. J. Inorg. Chem.*, 2017, **2017**(8), 1180–1188, DOI: 10.1002/ejic.201601404.

33 J. E. Kim, D. S. Weinberger, P. J. Carroll and E. J. Schelter, Synthesis, Structural Characterization, and Carbonyl Addition Reactivity of a Terminal Cerium (III) Acetylide Complex, *Organometallics*, 2014, **33**(21), 5948–5951.

34 R. D. Shannon, Revised effective ionic radii and systematic studies of interatomic distances in halides and chalcogenides, *Acta Crystallogr., Sect. A*, 1976, **32**(5), 751–767.

35 M. E. Garner, B. F. Parker, S. Hohloch, R. G. Bergman and J. Arnold, Thorium Metallacycle Facilitates Catalytic Alkyne Hydrophosphination, *J. Am. Chem. Soc.*, 2017, **139**(37), 12935–12938, DOI: 10.1021/jacs.7b08323.

36 M. Suvova, K. T. P. O'Brien, J. H. Farnaby, J. B. Love, N. Kaltsoyannis and P. L. Arnold, Thorium(IV) and Uranium(IV) trans-Calix[2]benzene[2]pyrrolide Alkyl and Alkynyl Complexes: Synthesis, Reactivity, and Electronic Structure, *Organometallics*, 2017, **36**(23), 4669–4681, DOI: 10.1021/acs.organomet.7b00633.

37 N. S. Settineri and J. Arnold, Insertion, protonolysis and photolysis reactivity of a thorium monoalkyl amidinate complex, *Chem. Sci.*, 2018, **9**(10), 2831–2841, DOI: 10.1039/C7SC05328B.

38 Y. Wang, C. Zhang, G. Zi, W. Ding and M. D. Walter, Preparation of a potassium chloride bridged thorium phosphinidiide complex and its reactivity towards small organic molecules, *New J. Chem.*, 2019, **43**(24), 9527–9539, DOI: 10.1039/C9NJ02269D.

39 G. T. Kent, X. Yu, C. Pauly, G. Wu, J. Autschbach and T. W. Hayton, Synthesis of Parent Acetylide and Dicarbide Complexes of Thorium and Uranium and an Examination of Their Electronic Structures, *Inorg. Chem.*, 2021, **60**(20), 15413–15420, DOI: 10.1021/acs.inorgchem.1c02064.

40 J. Vícha, J. Novotný, S. Komorovsky, M. Straka, M. Kaupp and R. Marek, Relativistic Heavy-Neighbor-Atom Effects on NMR Shifts: Concepts and Trends Across the Periodic Table, *Chem. Rev.*, 2020, **120**(15), 7065–7103, DOI: 10.1021/acs.chemrev.9b00785.

41 T. W. Hayton and J. Autschbach, Using NMR Spectroscopy to Evaluate Metal–Ligand Bond Covalency for the f Elements, *Acc. Chem. Res.*, 2025, **58**(3), 488–498, DOI: 10.1021/acs.accounts.4c00727.

42 K. C. Mullane, P. Hrobárik, T. Cheisson, B. C. Manor, P. J. Carroll and E. J. Schelter, 13C NMR Shifts as an Indicator of U–C Bond Covalency in Uranium(VI) Acetylide Complexes: An Experimental and Computational Study, *Inorg. Chem.*, 2019, **58**(7), 4152–4163, DOI: 10.1021/acs.inorgchem.8b03175.

43 A. J. Lewis, P. J. Carroll and E. J. Schelter, Stable Uranium(VI) Methyl and Acetylide Complexes and the Elucidation of an Inverse Trans Influence Ligand Series, *J. Am. Chem. Soc.*, 2013, **135**(35), 13185–13192, DOI: 10.1021/ja406610r.

44 O. Ordoñez, X. Yu, G. Wu, J. Autschbach and T. W. Hayton, Homoleptic Perchlorophenyl "Ate" Complexes of Thorium(IV) and Uranium(IV), *Inorg. Chem.*, 2021, **60**(16), 12436–12444, DOI: 10.1021/acs.inorgchem.1c01686.

45 O. Ordoñez, X. Yu, G. Wu, J. Autschbach and T. W. Hayton, Synthesis and Characterization of Two Uranyl-Aryl "Ate" Complexes, *Chem.–Eur. J.*, 2021, **27**(19), 5885–5889, DOI: 10.1002/chem.202005078.

46 L. A. Seaman, P. Hrobárik, M. F. Schettini, S. Fortier, M. Kaupp and T. W. Hayton, A Rare Uranyl(VI)–Alkyl Ate Complex [Li(DME)1.5]2[UO2(CH2SiMe3)4] and Its Comparison with a Homoleptic Uranium(VI)–Hexaalkyl, *Angew. Chem., Int. Ed.*, 2013, **52**(11), 3259–3263, DOI: 10.1002/anie.201209611.

47 E. A. Pedrick, P. Hrobárik, L. A. Seaman, G. Wu and T. W. Hayton, Synthesis, structure and bonding of hexaphenyl thorium(iv): observation of a non-octahedral structure, *Chem. Commun.*, 2016, **52**(4), 689–692, DOI: 10.1039/C5CC08265J.

48 L. A. Seaman, E. A. Pedrick, T. Tsuchiya, G. Wu, E. Jakubikova and T. W. Hayton, Comparison of the Reactivity of 2-Li-C6H4CH2NMe2 with MCl4 (M=Th, U): Isolation of a Thorium Aryl Complex or a Uranium Benzyne Complex, *Angew. Chem., Int. Ed.*, 2013, **52**(40), 10589–10592, DOI: 10.1002/anie.201303992.

49 P. Hrobárik, V. Hrobáriková, A. H. Greif and M. Kaupp, Giant Spin-Orbit Effects on NMR Shifts in Diamagnetic Actinide Complexes: Guiding the Search of Uranium(VI) Hydride Complexes in the Correct Spectral Range, *Angew. Chem., Int. Ed.*, 2012, **51**(43), 10884–10888, DOI: 10.1002/anie.201204634.

50 Starkey, L. S., 13C NMR Chemical Shifts, https://www.cpp.edu/~lsstarkey/courses/NMR/NMRshifts13C.pdf, accessed.

51 P. Pandey, X. Yu, G. B. Panetti, E. Lapsheva, M. R. Gau, P. J. Carroll, J. Autschbach and E. J. Schelter, Synthesis, Electrochemical, and Computational Studies of Organocerium(III) Complexes with Ce–Aryl Sigma Bonds, *Organometallics*, 2023, **42**(12), 1267–1277, DOI: 10.1021/acs.organomet.2c00384.

52 H. H. Wilson, X. Yu, T. Cheisson, P. W. Smith, P. Pandey, P. J. Carroll, S. G. Minasian, J. Autschbach and E. J. Schelter, Synthesis and Characterization of a Bridging Cerium(IV) Nitride Complex, *J. Am. Chem. Soc.*, 2023, **145**(2), 781–786, DOI: 10.1021/jacs.2c12145.

53 T. Cheisson, K. D. Kersey, N. Mahieu, A. McSkimming, M. R. Gau, P. J. Carroll and E. J. Schelter, Multiple Bonding in Lanthanides and Actinides: Direct Comparison of Covalency in Thorium(IV)- and Cerium(IV)-Imido Complexes, *J. Am. Chem. Soc.*, 2019, **141**(23), 9185–9190, DOI: 10.1021/jacs.9b04061.

54 A. J. Gremillion, J. Ross, X. Yu, P. Ishtaweera, R. Anwander, J. Autschbach, G. A. Baker, S. P. Kelley and J. R. Walensky, Facile Oxidation of Ce(III) to Ce(IV) Using Cu(I) Salts, *Inorg. Chem.*, 2024, **63**(21), 9602–9609, DOI: 10.1021/acs.inorgchem.3c04337.

55 O. Ordoñez, X. Yu, G. Wu, J. Autschbach and T. W. Hayton, Assessing the 4f Orbital Participation in the Ln–C Bonds of [Li(THF)4][Ln(C6Cl5)4] (Ln = La, Ce), *Inorg. Chem.*, 2022, **61**(38), 15138–15143, DOI: 10.1021/acs.inorgchem.2c02304.

56 A. N. Rodionov, G. V. Timofeyuk, T. V. Talalaeva, D. N. Shigorin and K. A. Kocheshkov, Infrared spectra of some acetylides of lithium, sodium, and potassium, *Bull. Acad. Sci. USSR, Div. Chem. Sci.*, 1965, **14**(1), 37–40, DOI: 10.1007/BF00854856.

57 P.-M. Pellny, F. G. Kirchbauer, V. V. Burlakov, W. Baumann, A. Spannenberg and U. Rosenthal, Reactivity of Permethylzirconocene and Permethyltitanocene toward Disubstituted 1, 3-Butadiynes: η4-vs η2-Complexation or C− C Coupling with the Permethyltitanocene, *J. Am. Chem. Soc.*, 1999, **121**(36), 8313–8323.

58 K. E. Lee, K. T. Higa, R. A. Nissan and R. J. Butcher, Synthesis, characterization, and structure of acetylenic gallium dialkylphosphides having the formula [(tert-Bu)(Me3SiC. tplbond. C) GaPR2] 2 (R= Et, iso-Pr, tert-Bu), *Organometallics*, 1992, **11**(8), 2816–2821.

59 H. Lang and D. Seyferth, Synthese und Reaktivität von Alkinyl-substituierten Titanocen-Komplexen/Synthesis and Reactivity of Alkyne Substituted Titanocene Complexes, *Z. Naturforsch. B*, 1990, **45**(2), 212–220.

60 J. Lorberth, Spaltung der zinn-stickstoffbindung: (phenylalkynyl)stannane, *J. Organomet. Chem.*, 1969, **16**(2), 327–331, DOI: 10.1016/S0022-328X(00)81124-9.

61 E. Jeffery and T. Mole, Some new associated (phenylethynyl) metallic and octynylmetallic compounds, *J. Organomet. Chem.*, 1968, **11**, 393–398.

62 K. E. Lee and K. T. Higa, Synthesis, characterization, and reactivity of new alkylgallium acetylides, *J. Organomet. Chem.*, 1993, **449**(1–2), 53–59.

63 G. Deacon and D. Wilkinson, Organolanthanoids. XII. Reactions of bis (cyclopentadienyl) ytterbium (II) with some diorganomercurials, *Inorg. Chim. Acta*, 1988, **142**(1), 155–159.

64 T. Dolzine, A. Hovland and J. Oliver, Intramolecular cyclization of dimethyl (1-pent-4-enyl)-silyllithium, *J. Organomet. Chem.*, 1974, **65**(1), C1–C3.

65 P. W. Seavill, K. B. Holt and J. D. Wilden, Electrochemical preparation and applications of copper (i) acetylides: a demonstration of how electrochemistry can be used to facilitate sustainability in homogeneous catalysis, *Green Chem.*, 2018, **20**(24), 5474–5478.

66 J. A. Branson, P. W. Smith, D.-C. Sergentu, D. R. Russo, H. Gupta, C. H. Booth, J. Arnold, E. J. Schelter, J. Autschbach and S. G. Minasian, The Counterintuitive Relationship between Orbital Energy, Orbital Overlap, and Bond Covalency in CeF62– and CeCl62, *J. Am. Chem. Soc.*, 2024, **146**(37), 25640–25655, DOI: 10.1021/jacs.4c07459.

67 Y. Qiao, H. Yin, L. M. Moreau, R. Feng, R. F. Higgins, B. C. Manor, P. J. Carroll, C. H. Booth, J. Autschbach and E. J. Schelter, Cerium(iv) complexes with guanidinate ligands: intense colors and anomalous electronic structures, *Chem. Sci.*, 2021, **12**(10), 3558–3567, DOI: 10.1039/D0SC05193D.

68 C. H. Booth, M. D. Walter, M. Daniel, W. W. Lukens and R. A. Andersen, Self-Contained Kondo Effect in Single Molecules, *Phys. Rev. Lett.*, 2005, **95**(26), 267202, DOI: **10.1103/PhysRevLett.95.267202**.

69 The electrochemistry of [M][Ce(TriNOx)=*N*-(3,5-(CF_3)2C_6H_3)] was measured in DME and the electrochemistry of Ce(TriNOx)-X was measured in DCM. The CeTMS and CePh in this article were measured in DCM.

70 C. Sandford, M. A. Edwards, K. J. Klunder, D. P. Hickey, M. Li, K. Barman, M. S. Sigman, H. S. White and S. D. Minteer, A synthetic chemist's guide to electroanalytical tools for studying reaction mechanisms, *Chem. Sci.*, 2019, **10**(26), 6404–6422, DOI: **10.1039/C9SC01545K**.

71 The redox potential from DPV was obtained from the average of reduction and oxidation peak voltage.

72 T. G. Appleton, H. C. Clark and L. E. Manzer, The trans-influence: its measurement and significance, *Coord. Chem. Rev.*, 1973, **10**(3), 335–422, DOI: **10.1016/S0010-8545(00)80238-6**.

73 B. J. Coe and S. J. Glenwright, Trans-effects in octahedral transition metal complexes, *Coord. Chem. Rev.*, 2000, **203**(1), 5–80.

74 K. Krogh-Jespersen, M. D. Romanelli, J. H. Melman, T. J. Emge and J. G. Brennan, Covalent Bonding and the Trans Influence in Lanthanide Compounds, *Inorg. Chem.*, 2010, **49**(2), 552–560, DOI: **10.1021/ic901571m**.

75 G. B. Deacon and C. M. Forsyth, A Half-Sandwich Perfluoroorganoytterbium(II) Complex from a Simple Redox Transmetalation/Ligand Exchange Synthesis, *Organometallics*, 2003, **22**(7), 1349–1352, DOI: **10.1021/om021039a**.

76 D. Freedman, J. H. Melman, T. J. Emge and J. G. Brennan, Cubane Clusters Containing Lanthanide Ions: (py)8Yb4Se4(SePh)4 and (py)10Yb6S6(SPh)6, *Inorg. Chem.*, 1998, **37**(17), 4162–4163, DOI: **10.1021/ic9805832**.

77 G. B. Deacon, T. C. Feng, B. W. Skelton and A. H. White, Organoamido-and Aryloxo-Lanthanoids. XI. Syntheses and Crystal Structures of $Nd(Odpp)_3$, $Nd(Odpp)_3(thf)$ and $[Nd(Odpp)_3(thf)_2]$*2 (thf)($Odpp^-$=2, 6-Diphenylphenolate): Variations in Intramolecular π-Ph-Nd Interactions, *Aust. J. Chem.*, 1995, **48**(4), 741–756.

78 E. O'Grady and N. Kaltsoyannis, On the inverse trans influence. Density functional studies of [MOX5]n− (M = Pa, n = 2; M = U, n = 1; M = Np, n = 0; X = F, Cl or Br), *J. Chem. Soc., Dalton Trans.*, 2002, (6), 1233–1239, DOI: **10.1039/B109696F**.

79 O. P. Lam, S. M. Franke, H. Nakai, F. W. Heinemann, W. Hieringer and K. Meyer, Observation of the Inverse Trans Influence (ITI) in a Uranium(V) Imide Coordination Complex: An Experimental Study and Theoretical Evaluation, *Inorg. Chem.*, 2012, **51**(11), 6190–6199, DOI: **10.1021/ic300273d**.

80 H. S. La Pierre, M. Rosenzweig, B. Kosog, C. Hauser, F. W. Heinemann, S. T. Liddle and K. Meyer, Charge control of the inverse trans-influence, *Chem. Commun.*, 2015, **51**(93), 16671–16674.

81 A. J. Lewis, K. C. Mullane, E. Nakamaru-Ogiso, P. J. Carroll and E. J. Schelter, The Inverse Trans Influence in a Family of Pentavalent Uranium Complexes, *Inorg. Chem.*, 2014, **53**(13), 6944–6953, DOI: **10.1021/ic500833s**.

82 L. C. Motta and J. Autschbach, Actinide inverse trans influence versus cooperative pushing from below and multi-center bonding, *Nat. Commun.*, 2023, **14**(1), 4307, DOI: **10.1038/s41467-023-39626-8**.

83 H. S. La Pierre and K. Meyer, Uranium–Ligand Multiple Bonding in Uranyl Analogues, [L═U═L]n+, and the Inverse Trans Influence, *Inorg. Chem.*, 2013, **52**(2), 529–539, DOI: **10.1021/ic302412j**.

84 J. R. Levin, W. L. Dorfner, A. X. Dai, P. J. Carroll and E. J. Schelter, Density Functional Theory as a Predictive Tool for Cerium Redox Properties in Nonaqueous Solvents, *Inorg. Chem.*, 2016, **55**(24), 12651–12659, DOI: **10.1021/acs.inorgchem.6b01779**.

85 Q. Yang, X. Yu, E. Lapsheva, P. Pandey, P. W. Smith, H. Gupta, M. R. Gau, P. J. Carroll, S. G. Minasian, J. Autschbach and E. J. Schelter, CCDC 2448118: Experimental Crystal Structure Determination, 2025, DOI: **10.5517/ccdc.csd.cc2n5gkw**.

86 Q. Yang, X. Yu, E. Lapsheva, P. Pandey, P. W. Smith, H. Gupta, M. R. Gau, P. J. Carroll, S. G. Minasian, J. Autschbach and E. J. Schelter, CCDC 2448119: Experimental Crystal Structure Determination, 2025, DOI: **10.5517/ccdc.csd.cc2n5glx**.

87 Q. Yang, X. Yu, E. Lapsheva, P. Pandey, P. W. Smith, H. Gupta, M. R. Gau, P. J. Carroll, S. G. Minasian, J. Autschbach and E. J. Schelter, CCDC 2448120: Experimental Crystal Structure Determination, 2025, DOI: **10.5517/ccdc.csd.cc2n5gmy**.